

OFFICE OF NAVAL RESEARCH

Grant N00014-89-J-1261

R&T Code 4131038

ONR Technical Report #20

Vibrational Spectroscopy of Molecules at Liquid/Liquid Interfaces

by

G. L. Richmond

In Press

Department of Chemistry
1253 University of Oregon
Eugene, OR 97403

June 1997

Reproduction in whole, or in part, is permitted for any purpose of the United States Government.

This document has been approved for public release and sale; its distribution is unlimited.

VIBRATIONAL SPECTROSCOPY OF MOLECULES AT LIQUID/LIQUID INTERFACES

G.L. Richmond

Department of Chemistry
University of Oregon
Eugene, OR 97403

Abstract

Measurement of the nonlinear vibrational spectrum of molecules at a liquid/liquid interface has recently been achieved by the use of total internal reflection sum frequency vibrational spectroscopy (TIR SFVS). This report describes this nonlinear optical technique and gives examples of the type of information which has been obtained about interfacial water and surfactants adsorbed at this interface. The surfactants examined include simple alkyl cationic and anionic surfactants commonly used in cleaning products, and phosphatidylcholines which comprise the major component of cell membranes. Studies of interfacial water involve comparative studies at air/water and oil/water interfaces, and the effect of adsorbed surfactant on the water structure and orientation at these two interfaces.

Introduction

Liquid surfaces and interfaces play a central role in many of the chemical and physical processes in our everyday lives. Exchange of molecules and ions across liquid or membrane surfaces is prevalent in biological processes. Many environmentally important chemical separation processes are based upon the partitioning of solute molecules across the interface between two immiscible liquids. Respiration in the lungs of living organisms occurs across lipid surfactant monolayers. The ordering of organic molecules at liquid interfaces to form supramolecular structures upon transfer to a solid are being used in molecular recognition, catalysis and nonlinear optical applications.

To understand such processes requires a knowledge of the structure and dynamics of these liquid interfaces on a molecular level. Our understanding of the properties of these interfaces has come primarily from theoretical studies and experimental measurements of a more macroscopic nature. The development of several experimental techniques has recently advanced our knowledge about molecular structure at liquid/air interfaces. Neutron¹ and x-ray² diffraction and reflection studies have provided structural details on an Angstrom level about molecular packing at the liquid/air interface. From optical techniques such as fourier transform infrared (FTIR),³ Brewster angle microscopy,⁴ fluorescence microscopy,⁵ sum frequency vibrational spectroscopy (SFVS)⁶⁻⁸ and second harmonic generation (SHG),⁸⁻¹¹ information about phase behavior and the structure and orientation of molecules at this interface has been obtained. Progress has been much slower in understanding the molecular structure at the interface between two bulk liquids because of inapplicability or lack of surface specificity of most surface techniques for probing this interface. Studies using fluorescent probes¹² that adsorb at this interface have been particularly useful as have resonant and nonresonant SHG studies.^{10,11,13,14}

In the past few years we have developed a means of measuring the vibrational spectra of molecules adsorbed at the interface between two immiscible liquids. Our success has come from application of technique called total internal reflection sum

frequency vibrational spectroscopy (TIR-SFVS)^{15,16} to this interface. The combination of the unique selectivity of SFVS to measure the molecular spectra of surface molecules and the enhanced sensitivity provided by the TIR geometry makes TIR-SFVS a powerful technique for measuring molecular structure at this interface. This report provides an overview of the technique, examples of the type of information obtainable and some thoughts about opportunities for future applications.

Principles of Sum Frequency Vibrational Spectroscopy

VSFS is a nonlinear optical method used to measure the vibrational spectrum of surface molecules with inherent discrimination against molecules in the adjacent bulk liquid. Pioneered by Shen,⁸ it is based upon the second order optical phenomena called sum frequency generation (SFG). SFG consists of illuminating the surface of a solid or liquid with two overlapping pulsed laser beams of different frequencies, ω_1 and ω_2 . At the surface, the intense optical fields induce a second order polarization of the medium at $\omega_1 \pm \omega_2$. This higher order polarization results in the production of a coherent optical field, which for SFG, is at the summed frequency. The surface sensitivity of SFG arises from the asymmetry of an interface relative to the adjacent bulk liquid, gas or solid. Under the electric dipole approximation, second order nonlinear optical processes are forbidden from occurring in bulk centrosymmetric media. Consequently, the characteristics of the SF response reflect the molecular properties of the interface.

Typically for SFVS, one of the laser beams is fixed at a visible frequency and the second is tunable within the infrared region of the spectrum of interest. (Fig. 1) Because of the relatively weak nature of this second order polarization, pulsed lasers are generally employed with the higher peak powers of shorter pulses preferred. The SF light produced at the interface occurs in both reflectance and transmittance at an angle a few degrees removed from the linear reflection and transmission angles.

Obtaining a vibrational spectrum of a molecule with SFG relies on an optical resonance between the tunable infrared beam, ω_{IR} , and the frequency of the vibrational transition in the molecule, ω_{v} . As ω_{IR} is tuned over a molecular resonance in the surface molecule of interest, the efficiency of the SFG process is correspondingly enhanced. There is always an additional nonresonant background contribution which for liquid surfaces and interfaces is usually quite small. The strength of the resonant SFG response depends upon several factors; the surface density of the molecule of interest, the line width of the transition, the IR transition moment, and the Raman transition strength. The last two factors restrict the technique to the study of vibrational modes which are *both* infrared and Raman active. Beyond the surface sensitivity, an additional advantage is that the detected SFV signal occurs in the visible region where detection optics are relatively efficient. Some of the disadvantages include low signal levels and difficulties in determining a quantitative relationship between the peak intensities and the number of molecules being sampled.

SFVS has been used to study a variety of liquid surface processes¹¹. To give a few examples, there have been a number of SFVS studies of monolayers at the air/water interface^{6,17,18} in addition to studies which report the VSF spectrum of water at the air/water interface,¹⁹ alcohols at the liquid/vapor interface,²⁰ and the surface of aqueous solutions of acetonitrile²¹. Many studies have been pursued which examine molecular adsorbates at metal and semiconductor surfaces in both ultra high vacuum, electrochemical and ambient environments.

Instrumentation and Experimental Considerations

In TIR VSFS studies of liquid/liquid interfaces the incident beams are sent through the higher index medium at the critical angle for each particular beam as shown in Fig. 1.¹⁵ For our experiments in which CCl_4 and H_2O or D_2O are used as the bulk liquids, the IR and visible beam are brought through the CCl_4 solution at the appropriate angles as determined by expressions given elsewhere.²² The VSF response is collected in reflection

at the corresponding critical angle for the sum frequency. We find that the enhancement in the SF response using the TIR geometry is 4-5 orders of magnitude higher than what we obtain using an external reflection geometry. This enhancement has allowed us to work with relatively low incident photon densities, minimizing the risk of thermal heating. We have found a similar enhancement in the TIR SHG response which has been useful in studies of alkane/water interfaces¹⁴ and the interface between two immiscible electrolyte solutions.¹³

One of the current limitations of the technique is the availability of nanosecond or picosecond IR laser sources which are broadly tunable over the infrared region. Most studies to date have been restricted to regions of the IR where tunable laboratory laser sources are available. We provide two examples here of laser systems which we have found to be quite successful in the 2-4 micron region. The simplest system as shown in Figure 1 consists of a LiNbO₃ optical parametric oscillator (OPO) which is pumped with the fundamental output of a Q-switched Nd:YAG laser generating 1064 nm pulses at 10 Hz with a pulse duration of 12 ns. Tunability throughout the desired wavelength region is achieved by angle tuning the LiNbO₃ crystal. IR light pulses in the 2700-3100 cm⁻¹ region with a bandwidth of 6 cm⁻¹ and energies of 2-3 mJ are obtainable over this spectral region. The visible probe beam is the remainder of the 1064 nm YAG fundamental which is frequency doubled to generate 532 nm. The advantages of this system lies in its relatively low cost and low maintenance. The disadvantage is in the limitation of the wavelength region accessible. Other Nd:YAG pumped IR laser systems have also been used in this region which vary in the pulse duration of the pump laser and nonlinear crystals used.^{6,11,18,23}

An alternate system that we are also using offers more promise for future extended wavelength tunability. It consists of a Ti:Sapphire regenerative amplifier laser system which is used to pump a two-stage optical parametric amplifier (KTP) seeded with a small portion of white light continuum.²⁴ This system currently produces IR pulses tunable from

2.4 to 4.0 μm at a repetition rate of 1 kHz. The energy of the pulses over this range is approximately 10 μJ with a bandwidth of 18 cm^{-1} and a pulse duration of 1.9 ps. The IR pulses are combined at the interface with the 800 nm light from the Ti:sapphire regenerative amplifier. With appropriate optics, the bandwidth of this laser can be readily narrowed. More importantly, with the use of other nonlinear crystals to generate infrared light, one should be able to probe vibrational transitions from 1-8 μm .

The studies conducted thus far in our laboratory have focussed on molecules studied at a $\text{CCl}_4/\text{H}_2\text{O}$ or $\text{CCl}_4/\text{D}_2\text{O}$ interface. This is the simplest oil/water system to study from a spectroscopic viewpoint because of the transparency of the CCl_4 to the infrared wavelengths accessible with our laser systems. The spectroscopic measurements are complemented by surface tension measurements made for example by the Wilhelmy plate method.

Examples of Simple Ionic Surfactants

The production of surfactants has increased tremendously over the past two decades with the rise in applications of these molecules. Although the bulk of surfactants produced is still used for conventional purposes such as washing and cleaning, they are also widely used in the stabilization of foams and emulsions for processing beverages and foodstuffs, in the stabilization of particulate dispersions and in secondary recovery of oil from porous rock beds. All of these uses depend upon the amphiphilic character of the molecule comprised of a nonpolar hydrophobic hydrocarbon portion and a polar hydrophilic portion. The need to satisfy the conflicting characteristics of the molecule and minimize the energy of the system leads to a host of complex structural features of these molecules in the bulk solution (eg. micelles and vesicles) as well as at interfaces where they can form monolayers of different phases.

When a surfactant adsorbs at an oil/water interface, the hydrophilic portion, or head group, remains in the aqueous phase while the hydrophobic end, or tail, is solvated by the

oil phase. Although much has been learned in recent years about how variations in the hydrophilic and hydrophobic portion of the molecules lead to different structural features at the air/water interface, little is known about their behavior at the more complex oil/water interface. For example, what effect does the nonpolar solvent have upon the van der Waals interactions between the hydrophobic alkyl chains of the molecule as the solvent penetrates into the chain structure? At an air/water interface, such attractive forces can counter the repulsion between the similarly charged head groups at the interface. What type of balance between these two effects is struck at the oil/water interface? In an attempt to understand such effects we have examined a range of common anionic and cationic alkyl surfactants by TIR SFVS and corresponding surface tension measurements. The results for two simple alkyl surfactants are described below to provide examples of the type of information learned in these spectroscopic studies.

Anionic surfactants hold the largest share of surfactant demand throughout the world. Of these, sodium dodecyl sulfate (SDS) is probably the most frequently studied surfactant and exists in a range of commercial products. Cationic surfactants, specifically the ammonium salts, play an important role as sanitizing and antiseptic agents, germicides, fungicides and as components in many cosmetic formulations. Figure 2 shows the vibrational spectra SDS and dodecylammonium chloride (DAC) at the $\text{CCl}_4/\text{D}_2\text{O}$ interface obtained by employing the Nd:YAG pumped OPO system described above.^{15,16,25} The S_{sfg} , S_{vis} , P_{IR} polarization combination has been used here to probe SF active vibrational modes that have transition moments with components perpendicular to the plane of the surface. The spectra depicted correspond to bulk surfactant concentrations where interfacial coverages have reached a maximum (referred to here as a monolayer) as indicated by the interfacial tension measurements. Both surfactants are soluble in the aqueous phase and are at concentrations (5.0 mM) below the critical micelle concentration for each of the surfactants. Spectra of comparable S/N have been obtained for these surfactants at interfacial coverages down to 0.05 monolayer. Using the Ti:sapphire pumped OPO system

with the shorter pulse duration, our sensitivity improves by 2-3 orders of magnitude. The spectral features represent the C-H stretching modes of the methylene units in the backbone of the 12 carbon alkyl chain of the amphiphiles and the terminal methyl group. The methylene asymmetric stretch contributes to the strong intensity at 2930 cm^{-1} . Peaks of moderate intensity are observed for the methylene symmetric and methyl symmetric stretches near 2850 cm^{-1} and 2872 cm^{-1} respectively. Assignments of the spectral features have been confirmed by selective deuteration studies.²⁶

To ascertain the relative order of the alkyl chains of these molecules at this and other surface concentrations, the intensities of the methyl and methylene symmetric stretch peaks in the SFG spectra are examined. The local symmetry of the CH_2 hydrocarbon backbone plays an important role in the determination of peak intensities of the CH_2 resonances. Under the electric dipole approximation for SFG, negligible contribution from methylene resonances should be observed for a system of well-ordered (all-*trans*) hydrocarbon chains.¹⁷ As more *gauche* defects are introduced into the alkyl chain, the intensity of the methylene modes would be expected to increase as local symmetry constraints are relaxed. This makes the methyl and methylene region of the SF spectrum an especially sensitive indicator of alkyl chain conformation. A schematic of the transition moments for the symmetric methyl and methylene modes for both *gauche* and *trans* conformations are illustrated in Figure 3. The presence of a significant methylene intensity (2850 cm^{-1}) in both the SDS and DAC at this maximum interfacial coverage suggests a significant number of *gauche* defects in the hydrocarbon chain.

The terminal methyl group, which possesses both IR and Raman active vibrational modes, is by nature in a noncentrosymmetric environment. Conformational information can be obtained from the relative intensity of the methyl peaks which reflect the orientational average of the ensemble with respect to the surface normal. By judicious choice of the polarization of the incident optical beams, and selection of appropriate output polarizations, the polarization dependence of the symmetric methyl stretch has been used as

a means of determining the average tilt angle of the hydrocarbon chain in these systems.¹⁷ For both SDS and DAC, polarization studies show the terminal methyl group to point on the average along the surface normal.²⁶ The orientation angle of specific bonds in the molecule of interest has been used frequently in previous studies.^{11,17,27} There are however some limitations to these measurements due to the low signal levels for some polarization combinations used to determine bond orientation.⁶

To understand how the conformational order of the alkyl chains varies with surface concentration, the ratio of the intensities of the symmetric methyl and symmetric methylene stretch mode have been used in many VSFS studies as an indicator of the relative order within the hydrocarbon chains.^{6,11,17,25} A low methyl to methylene ratio reflects a relatively large number of *gauche* defects in the alkyl chain. In our studies of charged alkyl surfactants adsorbed at the CCl₄/H₂O interface we consistently find that the greatest number of *gauche* defects are present at the lower interfacial concentrations. Increasing ordering of the alkyl chains is observed as the interfacial density of the surfactant increases. However, even at the highest interfacial coverages, all surfactants examined show significant alkyl chain disorder contrary to what is observed for many monolayers at solid/air and liquid/air interfaces where the van der Waals interactions between the hydrophobic tails play an important role in monolayer stability. Furthermore, unlike many Langmuir layers at solid/air and liquid/air interfaces, we find the ordering of the chains to be indistinguishable for surfactants of consecutive even/odd chain lengths, providing additional evidence of the disruptive nature of the solvent on the van der Waals interactions between chains.

Interestingly, the cationic surfactants studied including dodecyltrimethylammonium chloride consistently show a higher degree of alkyl chain ordering than the anionic surfactants when compared at similar surface concentrations.²⁶ Differences in their amphiphilic behavior is also manifested in their critical micelle concentrations, which for example, are 8.2 mM and 14.0 mM for SDS and DAC respectively. Since the surfactant molecular interactions in a micelle environment have many similarities with surfactants at an

oil/water interface, it is hoped that eventually one might be able to use liquid/liquid interfacial studies such as these to understand interactions in micelles and other structures in the bulk liquid.

Interfacial Water Structure and Orientation

Knowledge of the molecular properties of water at liquid interfaces and organized assemblies is a prerequisite for understanding a variety of interfacial processes such as chemical reactivity, equilibria, proton transfer and ion exchange. Recent research suggests that the most fundamental aspects of wetting phenomena are guided to a large extent by the structure and molecular properties of interfacial water. Structural features of interfacial water determine the nature of interaction forces which control flocculation, preparation of thin films and dispersions and emulsions. Solvation can have a large effect on the rates of certain surfactant reactions and can participate as an interfacial reactant in spontaneous hydrolysis of numerous organic species such as acyl chlorides, acid anhydrides and organic and inorganic esters.

We have recently measured the first vibrational spectrum of water molecules at the interface between two bulk immiscible liquids.²⁸ The results demonstrate that (1) the vibrational spectrum of water can be readily obtained at the oil/water interface using the TIR VSFS geometry, (2) the presence of the CCl₄ layer results in increased hydrogen bonding between water molecules at the interface relative to the air/water interface. These experiments have employed the Ti:sapphire pumped OPA system so that the OH and OD vibrational stretches of H₂O and D₂O can be accessed.²⁴ Figure 4(a) shows a comparison of the vibrational spectrum of interfacial water at the air/water and CCl₄/H₂O interface.²⁸ For the air/water interface, as measured previously by Shen and coworkers,¹⁹ we find that two peaks are prominent in the O-H stretching region studied here. The largest one at 3200 cm⁻¹ corresponds to the coupled OH symmetric stretch from tetrahedrally coordinated water molecules at the interface (OH-SS-S). At a quartz/ice interface, this "ice-like" peak dominates the VSF spectrum.¹⁹ The second peak at 3450 cm⁻¹ (labeled as OH-SS-A) is

attributed to molecular arrangements of more "liquid-like" water that has incomplete tetrahedral coordination (lower degree of hydrogen bonding). In contrast, the spectrum of water at the $\text{CCl}_4/\text{H}_2\text{O}$ interface shows a dominance of the "ice-like" peak with an absence of any measurable signal from the higher energy mode. This suggests that the presence of the CCl_4 results in increased hydrogen bonding between interfacial molecules, the hydrophobic liquid phase placing a physical restriction on the water molecules. The small peak near 2950 cm^{-1} is due to unavoidable minute traces of impurities in the solvent that concentrate over time at the interface. That the trace amounts of impurity can be seen at the $\text{CCl}_4/\text{H}_2\text{O}$ interface but not at the air/water interface is a result of the heightened sensitivity to interfacial structure and adsorbate concentration that the TIR geometry provides.

Effect of adsorbed surfactants on the interfacial water orientation

Another direction that we have taken the VSFS studies is towards understanding how the structure and orientation of interfacial water is affected by the presence of charged surfactants.^{7,29} The vibrational structure of both the interfacial water molecules and adsorbed surfactant are probed in these studies as increasing amounts of surfactants are added to the aqueous phase. Figure 4(b) shows the SFV spectrum from of SDS at the $\text{CCl}_4/\text{H}_2\text{O}$ interface. In the C-H stretching region of $2600 - 3000\text{ cm}^{-1}$, the response is similar to what was seen previously for SDS and DAC where considerable *gauche* defects in the alkyl chains are apparent by the strong symmetric methylene contribution near 2850 cm^{-1} .^{16,26} The peaks widths are different than in the previous spectra (Figure 2) because of the wider bandwidth of the Ti:sapphire system. The most striking result from these studies occurs in the O-H stretch region corresponding to interfacial water. With increased surfactant concentration, a strong enhancement in the "ice-like" peak is observed relative to the surfactant free interface. For similar studies of SDS studied at the air/water interface both the peaks shown in fig. 4 (a) are enhanced as the surfactant adsorbs.⁷ Polarization

studies show that these OH modes have a preferred orientation which is parallel to the surface normal.

We attribute this enhancement primarily to increased orientation of water molecules in the double layer region which is induced by this large electrostatic field created by the charged surfactant and counterion. Ionic strength studies support this conclusion. With increasing amounts of NaCl added, a decreased response from the O-H bands is observed. This can be understood in terms of a screening length which limits the number of interfacial water molecules that can interact with the electrostatic field as the ionic strength is increased.²⁹ In the presence of the field, the depth sampling of the optical fields in the water surface region is on the order of the double layer region, or the screening length. As this screening length is reduced with higher ionic strength, the number of aligned water molecules is reduced as manifested in the reduced OH response.

Some general trends have emerged from these air/water and oil/water studies of interfacial water. For an uncharged surfactant such as pentadecanoic acid where the field in the double layer is minimal, the OH modes are barely detectable relative to signal in the methyl stretch region suggesting more random orientation of water molecules. For charged surfactants of different signs, the spectral features show that the water aligns in opposite directions depending upon whether the surfactant head group is cationic or anionic.⁷ This difference in alignment is manifested in an optical interference between C-H stretching modes and the OH symmetric stretch mode. This interference is constructive for the anionic surfactants and destructive for cationic surfactants, indicative of a change in phase of the OH response for the two different water orientations. For mixed surfactants where equal numbers of cationic and anionic surfactants are present, the OH enhancement does not occur indicating a minimal field alignment of the water molecules due to the reduced electrostatic field.

Studies of Phospholipids

Another class of surfactants that we have been investigating are phosphoglycerides. Phosphoglycerides, commonly referred to as phospholipids, form an interesting class of surfactants which comprise the major component of cell membranes. These biologically important surfactants are generally composed of di-fatty acid, monophosphoric acid esters of glycerol combined with a polar head group which can be charged or uncharged. Unlike the surfactants described above, these are generally insoluble in the bulk aqueous phase. Displaying good oil solubility, these molecules have found extensive commercial application as nonaqueous emulsifiers, dispersants, and wetting agents in inks, foods and cosmetics. Their unique molecular structure leads to the formation of interesting bilayer and vesicle structures in the bulk aqueous solution.

One particularly interesting class of phospholipids are the phosphatidylcholines (PC). The polar head group of these molecules consist of a negatively charged phosphate and a positively charged amine. At neutral pH, they exist as zwitterions with an ionizable negative charge on the phosphate and a positive charge on the ammonium ion. How these molecules might orient and order at an oil/water interface has been the focus of many theoretical studies over the past two decades but experimental data to validate these predictions have been few.

The phosphocholines examined most extensively in our laboratory consist of saturated, symmetric, dialkyl species having alkyl chain lengths of 12 carbon atoms (dilauroyl-PC or DLPC), 14 carbon atoms (dimyristoyl-PC, DMPC), 16 carbon atoms (dipalmitoyl-PC or DPPC) and 18 carbon atoms (distearoyl-PC or DSPC).³⁰ The aqueous phase is prepared by dissolving a given phosphocholine in a pH of 7.0 D₂O-phosphate buffer solution. The phospholipid suspension is sonicated above the liquid bilayer gel-liquid crystal phase transition temperature, a procedure that results in the creation of unilamellar vesicles in the bulk aqueous phase.³¹ When these vesicles approach the CCl₄/D₂O interface, they should break apart to form monolayers at the interface (Figure 5) by a mechanism which currently remains largely unclear.

At room temperature, the SFV spectra and the surface pressure measurements show that the shortest chain phospholipid (DLPC) has the greatest surface activity and also displays the highest degree of conformational alkyl chain ordering throughout the concentration range studied. At its terminal interfacial pressure, the DLPC monolayer exhibits the closest packing with a molecular area of approximately $50 \text{ \AA}^2/\text{molecule}$. From the intensities of the C-H stretching modes in the VSF spectra, the dialkyl chains show a relatively high degree of ordering at this maximum coverage with less population of *gauche* defects than any of the simple dodecyl surfactants discussed above. However, the strong methylene contribution at this interfacial concentration shows that the monolayers are not in an all-*trans* conformation. DMPC with its expanded monolayer ($70 \text{ \AA}^2/\text{molecule}$) shows somewhat less surface activity and a corresponding lower degree of conformational order than DLPC. The least surface active PCs are found to be DPPC and DSPC which form the least ordered - and most expanded - monolayers.

Why phospholipids differing in only the length of their hydrocarbon chains exhibit such different behavior is intriguing. We believe that the answer lies in the physical properties of the different phosphocholine vesicles in aqueous solution. When fully hydrated, phospholipids spontaneously form vesicles, uni or multilamellar bilayer structures.³¹ Two phases of vesicle lipid bilayers exist in the bulk phase, gel and liquid crystalline. Each phospholipid has a characteristic phase transition temperature, T_c , with the solid gel phase being the dominant bilayer structure at $T < T_c$ and the liquid crystalline phase present for $T > T_c$. DLPC has a T_c of -1°C . For the room temperature experiments presented above, the vesicle bilayers of DLPC exist in a disordered or liquid crystalline state, with relatively weak intermolecular forces between the hydrocarbon chains. DPPC and DSPC have T_c 's equal to 41°C and 55°C , respectively, meaning that vesicle bilayers of these PCs are in the well ordered, gel phase.

Our spectral and isotherm data suggest that monolayer structure is correlated with T_c ; a low T_c (e.g. -1°C for DLPC) leads to high interfacial concentration and a high degree

of order and vice versa. Temperature dependent studies confirm this. When the DSPC containing solution is prepared at a higher temperature above the T_c such that the vesicles are in their liquid crystalline form when monolayer formation at the $\text{CCl}_4/\text{D}_2\text{O}$ interface occurs, a more ordered monolayer is observed spectroscopically. Also at this higher temperature, a correspondingly higher interfacial pressure is measured which is comparable to the terminal pressure of DLPC at room temperature. Consistent results are also found for the DMPC and DPPC. These observations lead us to conclude that thermodynamics of monomer dissociation from the vesicles control the interfacial concentration and hence the structure of phospholipids adsorbed to the interface. Interestingly, it is found that with equivalent interfacial concentrations of the four phospholipids monolayers, the longer chain phospholipids, even when tightly packed, still sustain a greater number of gauche defects leading to a greater conformational disorder within the monolayer. This is opposite to the trend that we observe for these PCs at the air/water interface.

Additional studies of deuterated PCs have been conducted to isolate the response from C-H modes in the head group region of the phospholipids. The data is allowing us to learn about the head group orientation and environment of these phospholipids at the $\text{CCl}_4/\text{H}_2\text{O}$ interface. Studies of the structure and orientation of the water molecules at the interface in the presence of phospholipids have also been conducted. Less enhancement in the orientation of water in the double layer is observed relative to the alkyl surfactants as might be expected because of the zwitterionic nature of the PLs.

Future Potential

The results of these first vibrational spectroscopic studies of interfaces between two immiscible liquids show the valuable new insight which is possible using TIR SFVS. Because of the similarity between the interactions of surfactants at an oil/water interface and the molecular interactions between such amphiphiles in vesicles and micelles, spectroscopic studies such as these have the potential to provide much needed information about the structure of organized assemblies in the bulk solution.

The studies completed thus far are only the tip of the iceberg of what can be done in the future in studying molecular processes at this liquid-liquid interfaces. There are a host of surfactants which could readily be studied including other ionic surfactants, nonionic surfactants and polymers. With extended wavelength tunability to access other vibrational modes of the surfactants in the head group region, the potential exists to obtain a better understanding of solvation of the headgroup and its interfacial environment. By simultaneously measuring the spectrum of interfacial solvent molecules in the presence and absence of surfactants, a better picture of how the molecular structure of interfacial molecules affects the measured thermodynamic behavior of liquid/liquid interfaces should emerge. For biologically relevant molecules, studies in this area provide a means of obtaining a better understanding of bilayer formation and molecular assembly of molecules which have important relevance to a host of biologically important processes. The technique is readily adaptable for studying interfacial adsorption dynamics as well as the dynamics of photo-induced processes at liquid/liquid interfaces.

Acknowledgments:

The author acknowledges the National Science Foundation (CHE-9416856), the Office of Naval Research and the donors of the Petroleum Research Fund of the American Chemical Society for funding of the projects described in this paper. Additional thanks goes to D. E. Gragson and R.A. Walker for assistance in preparation of this manuscript.

Figure Captions:

Figure 1. Diagram of the experimental setup and cell design. The infrared (ω_{IR}) and the visible (ω_{VIS}) 532 nm beams are incident through the high index CCl_4 phase. Shown below the diagram is the Nd:YAG laser and the optical parametric oscillator(OPO) used to generate the IR pulses.

Figure 2. Schematic representation of the net transition dipole moment for the symmetric methyl and methylene vibrational modes for an all-*trans* and *gauche* conformation.

Figure 3. Sum-frequency vibrational spectrum of (a) SDS and (b) DAC at the $\text{CCl}_4/\text{D}_2\text{O}$ interface acquired with the polarization combination of *ssp* (*s* polarized SF, *s* polarized visible, *p* polarized IR). Bulk concentrations of the surfactants was 5.0 mM. The solid lines represent a fit to the spectra using a combination of Gaussian and Lorentzian functions for each peak.

Figure 4. Sum frequency vibrational spectra of (a) H_2O at the air/water interface (o) and the $\text{CCl}_4/\text{H}_2\text{O}$ interface (o) and (b) H_2O and SDS at the $\text{H}_2\text{O}/\text{CCl}_4$ interface with increasing concentrations of SDS added to the bulk aqueous phase. The spectra were taken with the Ti:sapphire pumped optical parametric oscillator with S_{sfg} , S_{vis} and P_{IR} polarizations.

Figure 5. Phospholipid vesicles in the aqueous phase break apart to form phospholipid monolayers at interfaces. Vesicles used in these studies are small unilamellar structures that result from sonication of aqueous phospholipid suspensions above the bilayer gel-liquid crystal phase transition temperature.

References

- (1) Lu, J. R.; Lee, E. M.; Thomas, R. K.; Penfold, J.; Flitsch, S. L., *Langmuir*, **1993**, *9*, 1353.
- (2) Shih, M. C.; Bohanon, T. M.; Mikrut, J. M.; Zschack, P.; Dutta, P., *Phys. Rev. A*, **1992**, *45*, 5374.
- (3) Buontempo, J. T.; Rice, S. A., *J. Chem. Phys.*, **1993**, *98*, 5835.
- (4) Fischer, B.; Tsao, M.-W.; Ruiz-Garcia, j.; Fischer, T. M.; Schwartz, D. K.; Knobler, C. M., *J. Phys. Chem.*, **1994**, *98*, 7430.
- (5) Qiu, X.; Ruiz-Garcia, J.; Stine, K. J.; Knobler, C. M.; Selinger, J. V., *Phys. Rev. Lett.*, **1991**, *67*, 703.
- (6) Bell, G. R.; Bain, C. D.; Ward, R. N., *J. Chem. Soc. Faraday Trans.*, **1996**, *92*, 515.
- (7) Gragson, D. E.; McCarty, B. M.; Richmond, G. L., *J. Phys. Chem.*, **1996**, *100*, 14272.
- (8) Shen, Y. R., *Nature*, **1989**, *337*, 519.
- (9) Richmond, G. L.; Robinson, J. M.; Shannon, V. L., *Prog. in Surf. Sci.*, **1988**, *28*, 1.
- (10) Corn, R. M.; Higgins, D. A., *Chem. Rev.*, **1994**, *94*, 107-125.
- (11) Eisenthal, K. B., *Chem. Rev.*, **1996**, *96*, 1343-1360.
- (12) Wirth, M. J.; Burbage, J. D., *J. Phys. Chem.*, **1992**, *96*, 9022.
- (13) Conboy, J. C.; Richmond, G. L., *J. Phys. Chem.*, **1997**, *101*, 983.
- (14) Conboy, J. C.; Daschbach, J. L.; Richmond, G. L., *J. Phys. Chem.*, **1994**, *98*, 9688.
- (15) Messmer, M.; Conboy, J. C.; Richmond, G. L., *J. Amer. Chem. Soc.*, **1995**, *117*, 8040.
- (16) Conboy, J. C.; Messmer, M. C.; Richmond, G. L., *J. Phys. Chem.*, **1996**, *100*, 7617.
- (17) Hunt, J. H.; Guyot-Sionnest, P.; Shen, Y. R., *Chem. Phys. Lett.*, **1987**, *133*, 189.
- (18) Wolfrum, K.; Laubereau, A., *Chem. Phys. Lett.*, **1994**, *228*, 83.
- (19) Du, Q.; Freysz, E.; Shen, Y. R., *Science*, **1994**, *264*, 826.
- (20) Stanners, C. D.; Du, Q.; Chin, R. P.; Cremer, P.; Somorjai, G. A.; Shen, Y.-R., *Chem. Phys. Lett.*, **1995**, *232*, 407.
- (21) Zhang, D.; Gutow, J. H.; Eisenthal, K. B.; Heinz, T. F., *J. Chem. Phys.*, **1994**, *98*, 5099.
- (22) Epperlein, D.; Dick, B.; Marowsky, G.; Reider, G. A., *App. Phys. B*, **1987**, *44*, 5.

- (23) Guyot-Sionnest, P.; Tadjeddine, A., *Langmuir*, **1990**, *5*, 172.
- (24) Gragson, D. E.; McCarty, B. M.; Richmond, G. L.; Alavi, D. S., *J. Opt. Soc. B*, **1996**, *13*, 1492.
- (25) Conboy, J. C.; Messmer, M. C.; Walker, R.; Richmond, G. L., *Progress in Coll. and Polym. Sci.*, **1997**, *103*, 10.
- (26) Conboy, J. C.; Messmer, M. C.; Richmond, G. L., *J. Phys. Chem.*, submitted.
- (27) Shen, Y. R., *Nature*, **1989**, *337*, 519.
- (28) Gragson, D. E.; Richmond, G. L., submitted.
- (29) Gragson, D. E.; McCarty, B. M.; Richmond, G. L., *J. Amer. Chem. Soc.*, **1997**, *119*, xxx.
- (30) Walker, R. A.; Conboy, J. C.; Richmond, G. L., *Langmuir*, **1997**, *19*, xxx.
- (31) Szoka, F.; Papahadjopoulos, D., *Annual Review of Biophysical Bioengineering*, **1980**, *9*, 467.

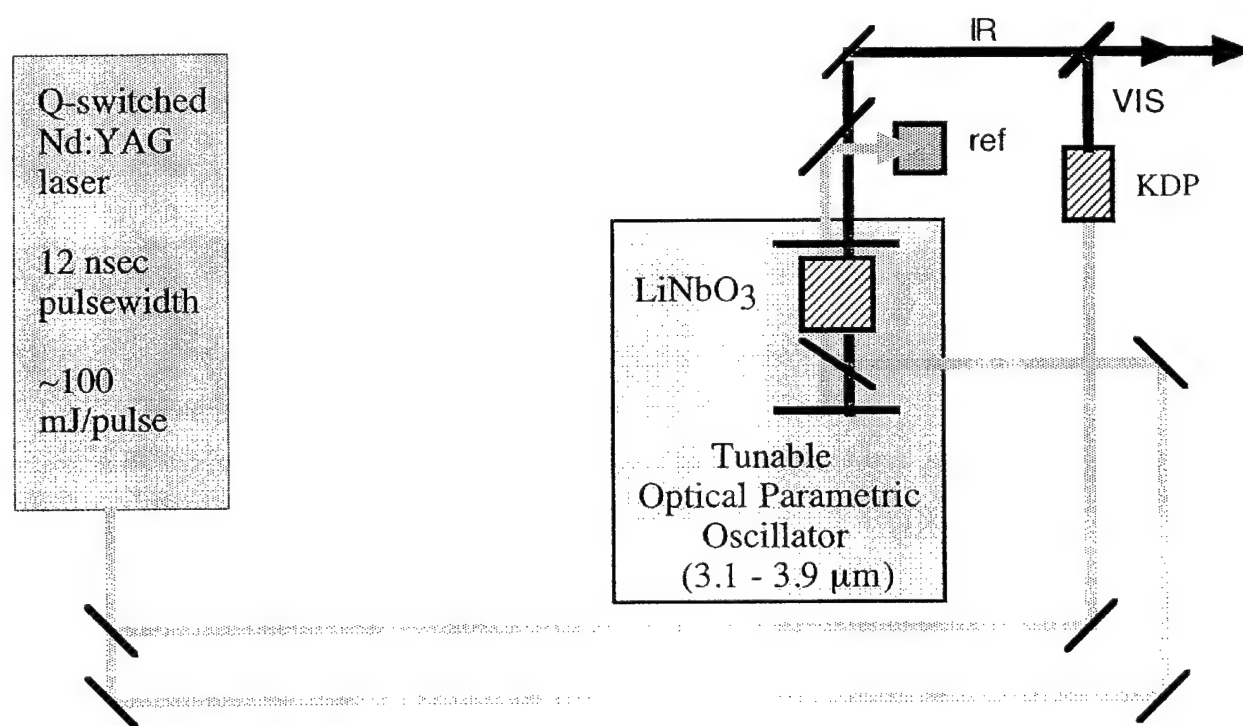
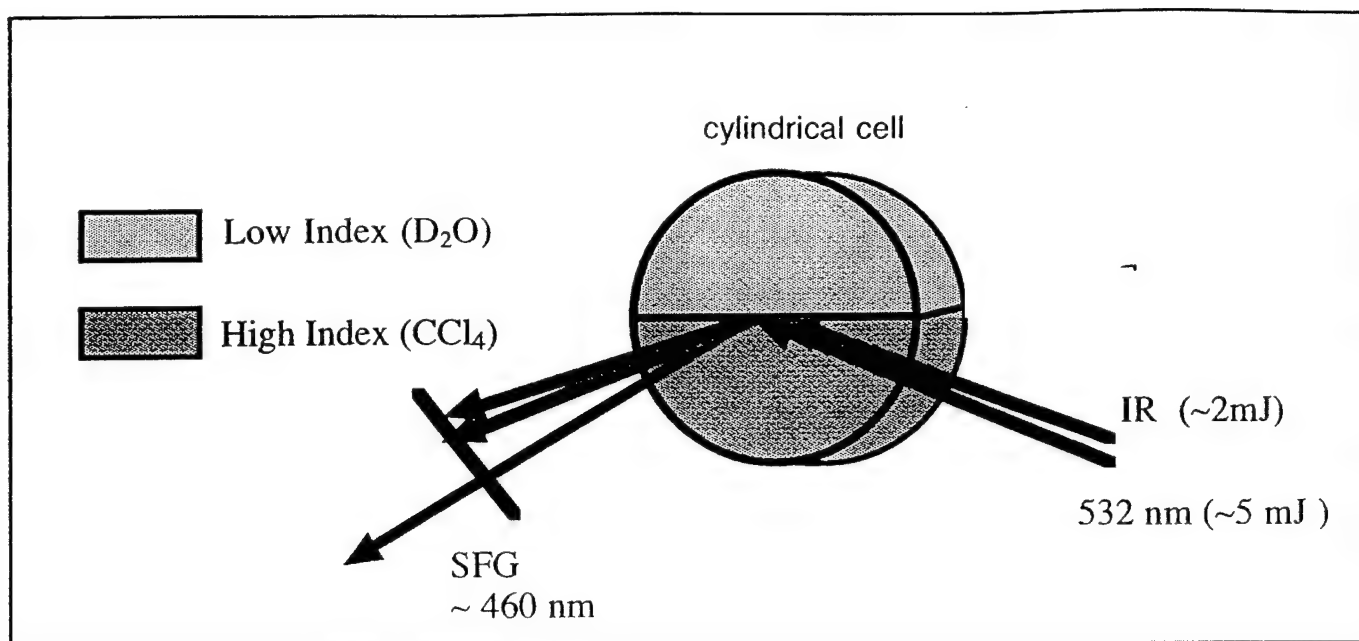


Figure 1

Figure 2

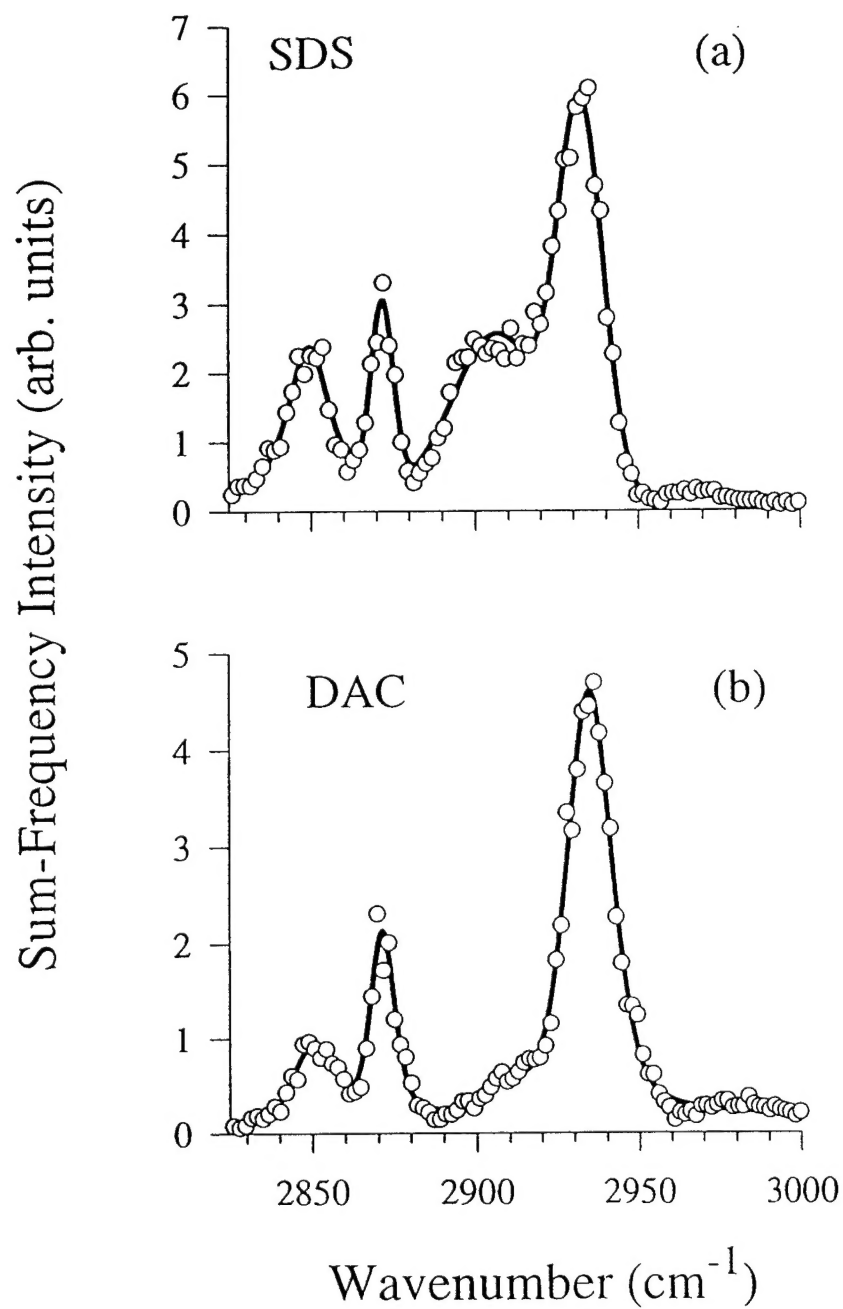
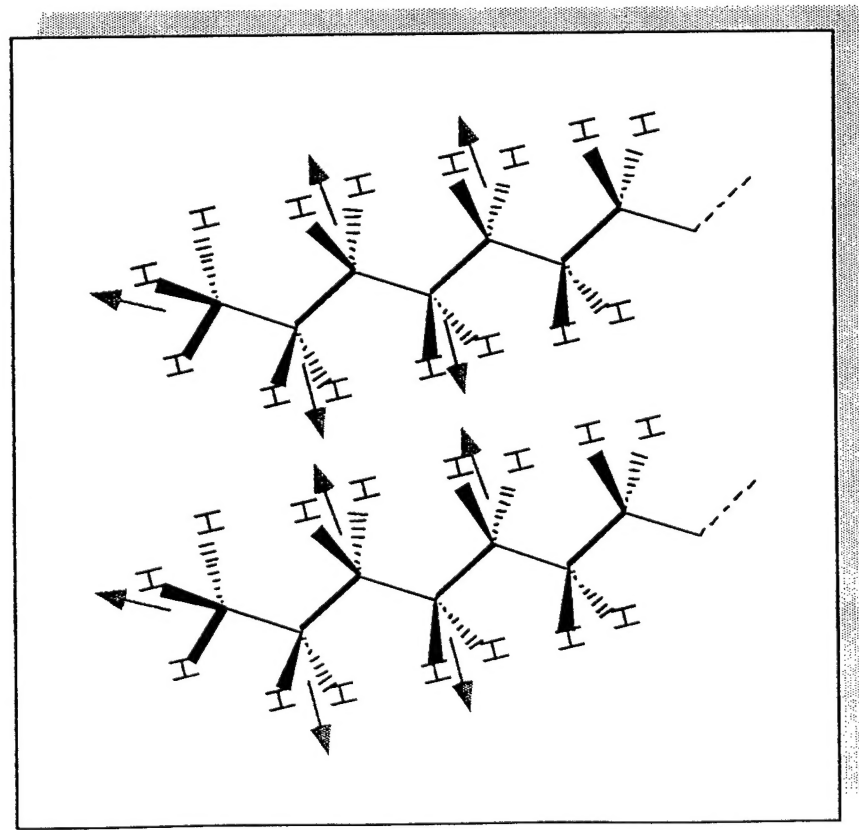
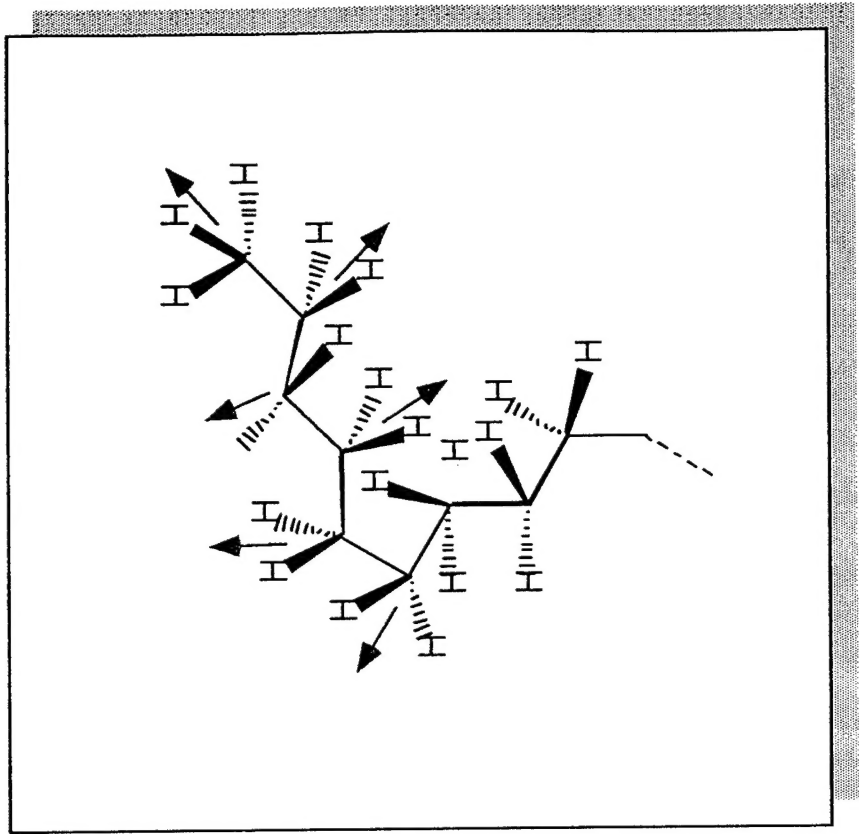


Figure 3



All-*trans* conformation



Gauche conformation

Figure 4

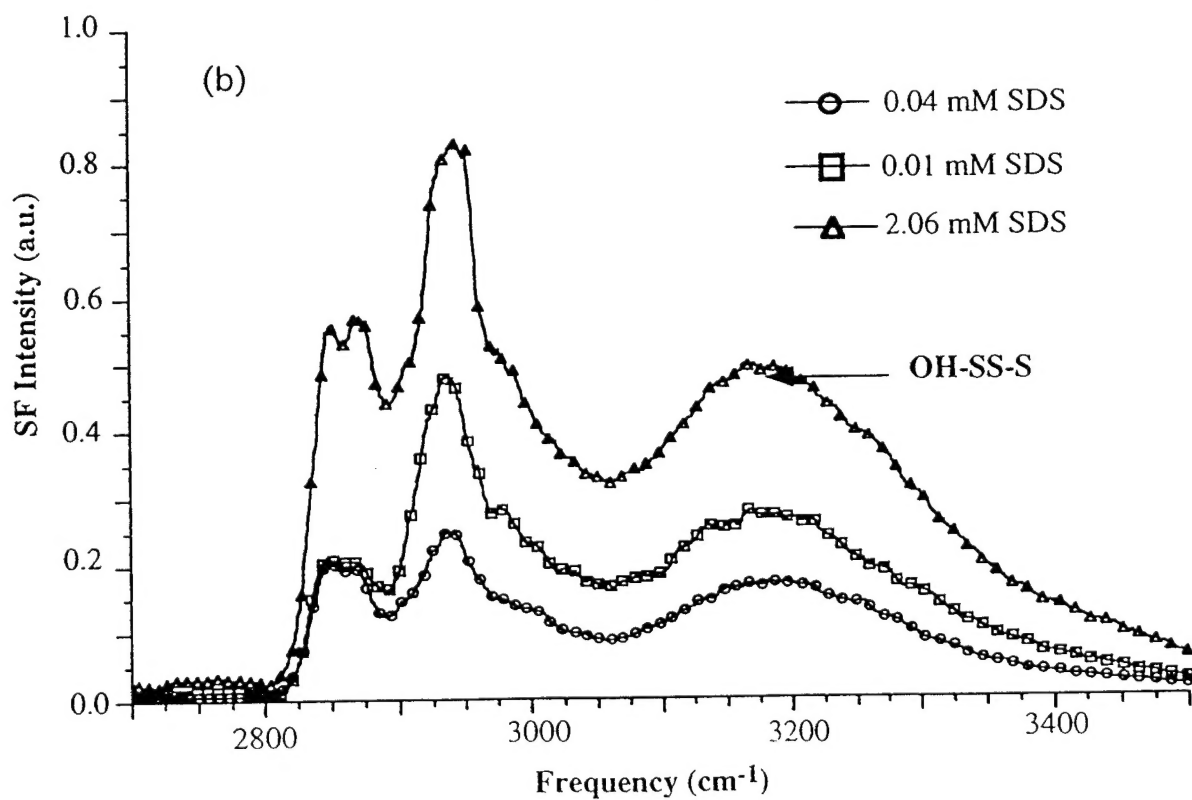
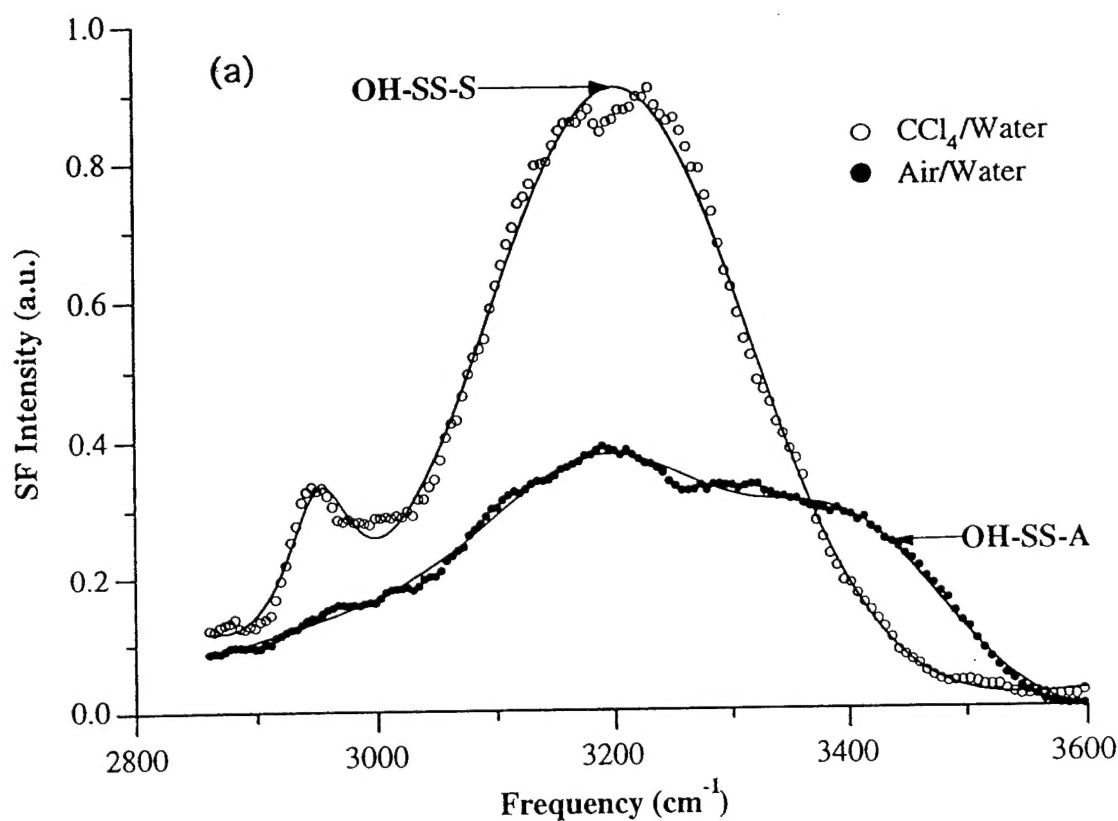


Figure 5

Vesicle decomposition at interfaces

